

# Trapped Ion Quantum Information Processing with Squeezed Phonons

Wenchao Ge,<sup>1,2</sup> Brian C. Sawyer,<sup>3</sup> Joseph W. Britton,<sup>1</sup> Kurt Jacobs,<sup>1,4,5</sup>

John J. Bollinger,<sup>6</sup> and Michael Foss-Feig<sup>1,7,8</sup>

<sup>1</sup>*United States Army Research Laboratory, Adelphi, Maryland 20783, USA*

<sup>2</sup>*The Institute for Research in Electronics and Applied Physics (IREAP), College Park, Maryland 20740, USA*

<sup>3</sup>*Georgia Tech Research Institute, Atlanta, Georgia 30332, USA*

<sup>4</sup>*Department of Physics, University of Massachusetts at Boston, Boston, Massachusetts 02125, USA*

<sup>5</sup>*Hearne Institute for Theoretical Physics, Louisiana State University, Baton Rouge, Louisiana 70803, USA*

<sup>6</sup>*National Institute of Standards and Technology, Boulder, Colorado 80305, USA,*

<sup>7</sup>*Joint Quantum Institute, NIST/University of Maryland, College Park, Maryland 20742, USA*

<sup>8</sup>*Joint Center for Quantum Information and Computer Science, NIST/University of Maryland, College Park, Maryland 20742, USA*



(Received 2 July 2018; published 24 January 2019)

Trapped ions offer a pristine platform for quantum computation and simulation, but improving their coherence remains a crucial challenge. Here, we propose and analyze a new strategy to enhance the coherent interactions in trapped ion systems via parametric amplification of the ions' motion—by squeezing the collective motional modes (phonons), the spin-spin interactions they mediate can be significantly enhanced. We illustrate the power of this approach by showing how it can enhance collective spin states useful for quantum metrology, and how it can improve the speed and fidelity of two-qubit gates in multi-ion systems, important ingredients for scalable trapped ion quantum computation. Our results are also directly relevant to numerous other physical platforms in which spin interactions are mediated by bosons.

DOI: [10.1103/PhysRevLett.122.030501](https://doi.org/10.1103/PhysRevLett.122.030501)

Trapped ions are among the best developed implementations of numerous quantum technologies, including quantum computers [1], quantum simulators [2], and quantum measurement devices [3]. For example, universal quantum gate sets have been implemented with extremely high fidelity in small systems [4,5], while quantum spin dynamics and entanglement generation have been demonstrated among tens [6] and even hundreds [7] of ions. For all of these applications, the general approach is to identify a qubit, i.e., two metastable atomic states, and then engineer interactions between qubits by controllably coupling them to the ions' collective motion (phonons), typically using lasers [1,8] or magnetic field gradients [9,10]. Putting aside the details of what specifically constitutes a qubit (hyperfine states of an ion, Rydberg levels of a neutral atom, charge states of a superconducting circuit), and what type of boson mediates interactions between them (phonons or photons), this basic paradigm of controllable boson-mediated interactions between qubits is at the heart of many physical implementations of quantum technologies. In all such systems, a key technical challenge is to make the interactions as strong as possible without compromising the qubit.

For trapped ions, the strength of interactions between qubits (from here forward called spins) is often limited by the available laser power or by the current that can be driven through a thin trap electrode. Where these technical limitations can be overcome, other more fundamental limits

remain. For example, the scattering due to the laser beams that generate spin-spin interactions can be the dominant source of decoherence [4,5,7], in which case using more laser power is not necessarily helpful [11–13]. Moreover, in many-ion strings larger laser power can lead to decoherence through off-resonant coupling to undesirable modes, a source of decoherence that becomes more severe with increasing ion number [14]. (Although this effect may be mitigated, it requires modulating the laser parameters in a complicated fashion [14–16].) In this Letter, we propose a straightforward experimental strategy to increase the strength of boson-mediated spin interactions that can also overcome the aforementioned limitations, and is sufficiently flexible to be relevant to numerous other systems in which qubits interact by exchanging bosons. In particular, we consider modulating the ions' trapping potential at nearly twice the typical motional mode frequency [17]. Related forms of parametric amplification (PA) of boson-mediated interactions have been considered recently in systems ranging from phonon-mediated superconductivity [18], to optomechanics [19] and cavity or circuit QED [20,21]. Our work goes further in that we determine the effects of PA in a driven multimode system, provide a simple physical explanation of its effects based on amplified geometric phases (see Fig. 1), and determine the capability of PA to enhance specific quantum information tasks performed with trapped ions.

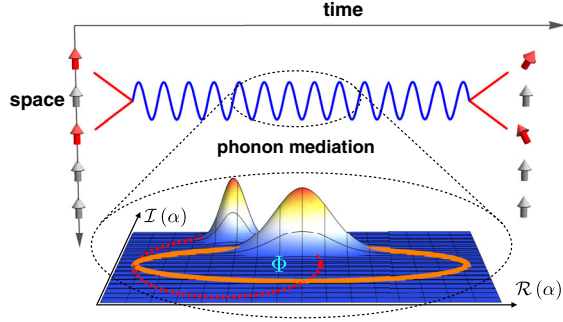


FIG. 1. Spin-spin interactions among trapped ions are mediated by phonon exchange, and their strength is proportional to the rate at which area ( $\Phi$ ) is enclosed by the phonon trajectories in phase space. The trajectories enclose area faster with parametric amplification (orange ellipse) than without (red dashed circle), leading to stronger spin-spin interactions.

Typically, spin-spin interactions between trapped ions are induced through spin-dependent acquisition of area swept out by phonon trajectories in phase space (Fig. 1). An area  $\Phi$  produces a multiplicative phase  $e^{-i\Phi}$  of the corresponding spin state, a geometric phase that depends only on the enclosed area [22–24]. The spin dependence can be achieved by driving the ions’ motion with a spin-dependent force (SDF), with characteristic interaction energy  $f$  (defined below). Once spin-dependent displacements have been seeded by the SDF, they can be amplified *spin independently* by modulating the trapping potential with a carefully chosen phase relative to the applied SDF (Fig. 1). Without PA, the time it takes to accumulate a particular geometric phase  $\Phi$ —corresponding to the generation of a particular entangled spin state—is lower bounded by  $t_{\min} \propto \sqrt{\Phi}/f$ . With PA this scaling is modified to

$$t_{\min} \propto \mathcal{S} \sqrt{\Phi}/f, \quad (1)$$

where  $\mathcal{S} < 1$  is the degree of squeezing in the squeezed mechanical quadrature, enabling a particular entangled state to be created faster for fixed laser power or magnetic field gradient.

*Trapped ion quantum simulators.*—Before describing the effects of PA, we briefly review the standard mechanism by which a trapped ion crystal with  $N$  ions can be made to simulate the quantum Ising model [2],

$$\hat{\mathcal{H}} = \hbar \frac{1}{N} \sum_{i < j} J_{ij} \hat{\sigma}_i^z \hat{\sigma}_j^z. \quad (2)$$

Here,  $\hat{\sigma}_i^z$  is the  $z$ -Pauli matrix for the  $i$ th ion, with the spin degree of freedom realized by two long-lived states.

In the Lamb-Dicke regime [25], the Hamiltonian describing an SDF oscillating at frequency  $\mu$  and with peak force  $F$  can be written in a frame rotating at  $\mu$  as [28,29]

$$\hat{\mathcal{H}}_{\text{SDF}} = \hbar \sum_{m=1}^N \left( f_m (\hat{a}_m + \hat{a}_m^\dagger) \sum_{i=1}^N U_{i,m} \hat{\sigma}_i^z - \delta_m \hat{a}_m^\dagger \hat{a}_m \right) + \hat{\mathcal{H}}_{\text{CR}}. \quad (3)$$

Here,  $f_m \propto F z_{0m}$  is the coupling strength of the SDF to the  $m$ th collective motional mode, with  $z_{0m} \equiv \sqrt{\hbar/2M\omega_m}$  the characteristic length scale of that mode,  $\omega_m$  its frequency, and  $M$  the ion mass. The  $U_{i,m}$  are matrix elements of the normal mode transformation matrix [30], and  $\delta_m \equiv \mu - \omega_m$ . The counterrotating Hamiltonian  $\hat{\mathcal{H}}_{\text{CR}}$  [25] can often be justifiably neglected in the rotating wave approximation (RWA).

There are two situations in which Eq. (3) reduces approximately to Eq. (2). If all of the modes are far off resonance ( $\delta_m \gg f_m$ ), they can be eliminated adiabatically to give the effective spin-spin interaction in Eq. (2) [25,31,32]. Alternatively, even if  $f_m \gtrsim \delta_m$  for a single mode, as long as all other modes are far off resonance then the spin state approximately disentangles from the motional state at times that are integer multiples of  $2\pi/\delta_m$ . At these times the spin-state evolution is the same as that given by Eq. (2), with  $J_{ij} \propto U_{i,m} U_{j,m} \times (N f_m^2 / \delta_m)$ . For example, if  $\mu$  is detuned close to the center of mass (COM) mode ( $m = 1$ ), then  $J_{ij} = J \equiv 2f_1^2/\delta_1$ , describing all-to-all interactions. (In what follows, we will drop the explicit subscripts on  $f$  and  $\delta$  when discussing a single mode.)

To understand the dependence of the geometric phase on the system parameters, we can consider the phase  $\Phi$  acquired by a single spin for simplicity. There is some freedom in how  $\Phi$  is generated, namely, the phonon trajectory can undergo any integer number of loops, each contributing  $4\pi(f/\delta)^2$  to  $\Phi$  and taking a time  $2\pi/\delta$ . At fixed  $f$ , reducing  $\delta$  decreases the time  $t$  required to generate  $\Phi$ , but  $\delta$  can only be reduced to the point where  $\Phi = 4\pi(f/\delta)^2$  because at least one loop must close. At this point,  $\delta_{\min} = f/\sqrt{\Phi/4\pi}$ , giving  $t_{\min} = 2\pi/\delta_{\min} \propto \sqrt{\Phi}/f$  as asserted above Eq. (1). In experiments that employ optical dipole forces to generate the SDF, the dominant decoherence source can be scattering from the laser beams that occurs at a rate  $\Gamma \propto f$  [12,29]. In such cases, preparation of a particular entangled spin state (corresponding to a particular  $\Phi$ ) is accompanied by the minimal accumulated decoherence  $\Gamma t_{\min} \propto \sqrt{\Phi}$ .

*Parametric amplification.*—We now consider what happens when the ion motion is parametrically amplified while simultaneously being driven by the SDF. If the PA is at twice the SDF frequency, then in a frame rotating at  $\mu$  the PA Hamiltonian is [17,25]

$$\hat{\mathcal{H}}_{\text{PA}} = \sum_m \hbar g_m \cos(2\mu t - \theta) (\hat{a}_m e^{i\mu t} + \hat{a}_m^\dagger e^{-i\mu t})^2. \quad (4)$$

Here,  $g_m = eV/(M\omega_m d_T^2)$ , with  $V$  the parametric drive voltage amplitude and  $d_T$  a characteristic trap dimension.

TABLE I. Rescaling of key quantities under PA.

	$\Phi$	$\tau$	$\alpha_m$
SDF only	$4\pi(f/\delta)^2$	$2\pi/\delta$	$2f/\delta_m$
SDF + PA	$4\pi(f/\delta)^2/(4\mathcal{S}^6)$	$(2\pi/\delta)/(2\mathcal{S}^2)$	$2f/(\delta_m - g)$

Typically,  $g_m$  depends weakly on  $m$ , and for simplicity we ignore the  $m$  dependence in what follows. Values of  $g$  as large as  $0.1 \times \omega_1$  appear feasible, in particular for traps with small  $d_T$ . The relative phase  $\theta$  between the PA and SDF can in principle be chosen at will. We assume  $\theta = 0$ , which is optimal; limitations imposed by fluctuations of  $\theta$  have been carefully analyzed and are discussed later.

At first inspection, evolution under both  $\hat{\mathcal{H}}_{\text{SDF}}$  and  $\hat{\mathcal{H}}_{\text{PA}}$  seems complicated.  $\hat{\mathcal{H}}_{\text{PA}}$  squeezes the motional state, while  $\hat{\mathcal{H}}_{\text{SDF}}$  entangles the spin and squeezed motional states in a complicated way. However, under the condition  $0 < g < \delta_m$  [33], each mode will still undergo a closed loop in phase space [34], returning to the initial unsqueezed motional state and disentangling from the spin state at integer multiples of  $2\pi/(\delta'_m)$ , with  $\delta'_m \equiv \sqrt{\delta_m^2 - g^2}$ . The total Hamiltonian can be written in a simple form by using a Bogoliubov transformation  $\hat{b}_m = \cosh r_m \hat{a}_m - \sinh r_m \hat{a}_m^\dagger$ , with  $r_m = -\log \mathcal{S}_m$  and  $\mathcal{S}_m = [(\delta_m - g)/(\delta_m + g)]^{1/4}$  [19]. In terms of these transformed operators,  $\hat{\mathcal{H}}_T = \hat{\mathcal{H}}_{\text{SDF}} + \hat{\mathcal{H}}_{\text{PA}}$  is given by

$$\hat{\mathcal{H}}_T = \hbar \sum_{m=1}^N \left( f'_m (\hat{b}_m + \hat{b}_m^\dagger) \sum_{i=1}^N U_{i,m} \hat{\sigma}_i^z - \delta'_m \hat{b}_m^\dagger \hat{b}_m \right) + \hat{\mathcal{H}}_{\text{CR}}, \quad (5)$$

where  $f'_m = f_m/\mathcal{S}_m$  and  $\hat{\mathcal{H}}_{\text{CR}}$  now contains the counter-rotating terms from both  $\hat{\mathcal{H}}_{\text{SDF}}$  and  $\hat{\mathcal{H}}_{\text{PA}}$  [25]. Therefore, we obtain a Hamiltonian that is identical (in the RWA) to  $\hat{\mathcal{H}}_{\text{SDF}}$  but with rescaled drive strengths and detunings. Although every mode is squeezed by PA, a single mode (we assume the COM mode) will dominate the dynamics if  $\delta - g \ll \delta_{m \neq 1} - g$ . Table I shows both the geometric phase  $\Phi$  and duration  $\tau$  of a single loop for the COM mode, along with the typical phase-space amplitudes  $\alpha_m$  of the other modes, in the limit that  $\delta - g \ll \delta + g$  (such that  $\delta' \approx 2\delta\mathcal{S}^2$ ). Note that  $\delta_m - g$  is bounded by the gap between the COM mode and its closest neighbor, so that residual displacements  $\alpha_m$  of the spectator modes are upper bounded as  $1/\mathcal{S}$  increases [25].

As argued above, without PA the fastest strategy for obtaining a particular geometric phase  $\Phi$  at fixed  $f$  is to choose  $\delta$  such that the COM mode undergoes a single loop, giving  $t_{\min} \propto \sqrt{\Phi}/f$ . With PA, we can similarly argue that the optimal strategy to obtain  $\Phi$  at fixed  $f$  and  $\mathcal{S}$  is to choose  $\delta$  such that a single loop is closed. Solving  $\Phi = 4\pi(f/\delta_{\min})^2/(4\mathcal{S}^6)$  for  $\delta_{\min}$  [and

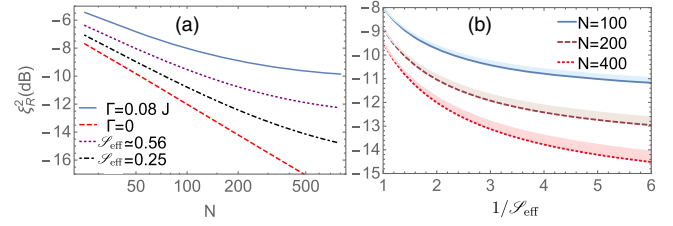


FIG. 2. Minimal squeezing  $\xi_R^2$  plotted (a) as a function of  $N$  for various situations; (b) versus  $1/\mathcal{S}_{\text{eff}}$  for several values of  $N$ , with shaded strips indicating the expected degradation of squeezing due to a phase uncertainty of  $\sigma_\theta = 18^\circ$ .

using  $t_{\min} = (2\pi/\delta_{\min})/(2\mathcal{S}^2)$  gives  $t_{\min} \propto \mathcal{S}\sqrt{\Phi}/f$ , as claimed in Eq. (1). Thus, we can generate the same spin state faster at fixed laser power or fixed current by reducing  $\mathcal{S}$ , which serves as a figure of merit for the benefits of PA. Physically, PA squeezes the phase-space loops into ellipses (see Fig. 1), which enclose more area (per unit time) for a fixed SDF. For the important situation where the SDF is generated by optical dipole forces and the decoherence rate  $\Gamma$  scales with the laser intensity, the accumulated decoherence can now be written as

$$\Gamma t_{\min} \propto \mathcal{S}\sqrt{\Phi}, \quad (6)$$

indicating that in principle the effect of decoherence in generating a particular entangled spin state can be made arbitrarily small. In practice there will be limits on  $\mathcal{S}$ , for example, due to the breakdown of the RWA (see Fig. 4). For the illustrations that follow, all results based on the RWA have been verified by numerically solving for the dynamics of  $\hat{\mathcal{H}}_T$ . In cases where the RWA is borderline, we then determine the reduction of the product  $f t_{\min}$  for fixed  $\Phi$  numerically [35], and report this reduction as the effective degree of squeezing  $\mathcal{S}_{\text{eff}}$ .

*Improving quantum spin squeezing.*—As an exemplary application of PA, we show how it improves quantum spin squeezing (QSS). QSS characterizes the reduction of spin noise in a collective spin system, and is important for both entanglement detection [36] and precision metrology [37]. Here, we investigate the Ramsey squeezing parameter  $\xi_R$  [38]; for coherent spin states,  $\xi_R^2 = 1$ , while for spin squeezed states  $\xi_R^2 < 1$  [37].

A simple way to realize QSS is via single-axis twisting [39], for which the ideal minimal squeezing parameter scales as  $N^{-2/3}$  for  $N \gg 1$  [37,39]. This limit is very challenging to achieve for large  $N$ . In fact, for decoherence attributable to spontaneous spin flips in the Ising ( $z$ ) basis at a rate  $\Gamma$  [12,40],  $\xi_R$  actually saturates for large  $N$  to the asymptotic value  $3[\Gamma/(2J)]^{2/3}$  [25,41], with the saturation taking place when  $N \gg 2J/\Gamma$ . To improve spin squeezing, the ratio  $J/\Gamma$  must be improved, which can be achieved via PA. To benchmark potential improvements, we analyze the effects of PA quantitatively under the experimental conditions in Ref. [7]. In Fig. 2(a), we plot the optimal spin



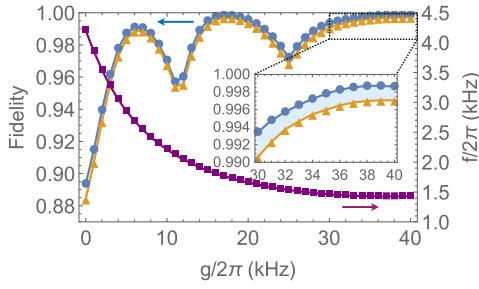


FIG. 3. Two-qubit gate fidelity in a 5-ion system, calculated from a numerical simulation of the full Hamiltonian  $\hat{H}_T$ . The optimal fidelity with (orange triangles) and without (blue dots) timing error (1%) as a function of the PA strength  $g$  for a gate time  $\tau \sim 180 \mu\text{s}$ . The purple squares correspond to the reduction of the laser power ( $f$ ) as the PA strength is increased.

squeezing as a function of  $N$ . The two outer lines represent SDF-only cases with (solid line) and without (dashed line) decoherence [42]. The two intermediate lines show how the decoherence-free results are approached as  $\mathcal{S}_{\text{eff}}$  is decreased. Figure 2(b) is similar to Fig. 2(a), but shows  $\xi_R^2$  as a function of  $1/\mathcal{S}_{\text{eff}}$  for different  $N$ .

*High fidelity two-qubit gate.*—Two-qubit gates with fidelity higher than 99.9% have recently been demonstrated in two-ion systems [4,5], where the largest remaining error is due to spontaneous emission from the driving lasers. Since a gate operation corresponds to some fixed  $\Phi$ , Eq. (6) implies that the effective spontaneous emission rate can be reduced by a factor of  $\mathcal{S}$  for a fixed gate time.

In many-ion systems, the gate time must be much longer than the inverse of the motional mode splitting in order to suppress gate errors due to spin-phonon entanglement with off-resonant modes [14]. If the gate time is reduced by using more laser power, then off-resonant modes experience larger phase-space excursions ( $\alpha_m \propto f$ ) and the fidelity suffers. By using PA, the gate time ( $\tau$ ) and the off-resonant loop size ( $\alpha_m$ ) are independent, and we can hold the gate time fixed while decreasing  $\alpha_m$  by a factor of  $\mathcal{S}$ . For example, comparing with the latest modulated pulsed laser scheme [16] that used  $f/2\pi = 10 \text{ kHz}$  for a two-qubit gate in a 5-ion chain, we calculate that our scheme can implement the same task with a comparable gate time ( $\tau \sim 180 \mu\text{s}$ ) and fidelity  $\geq 99.5\%$  using significantly less laser power (see Fig. 3) for the same trap frequency ( $\omega_1/2\pi = 3.045 \text{ MHz}$ ). As shown in Fig. 3, the fidelity can be improved by tuning  $g$  to minimize the total residual displacements [25]. With the access to larger  $g \sim 2\pi \times 100 \text{ kHz}$ , PA could enable a much faster two-qubit gate ( $\sim 30 \mu\text{s}$ ) with high fidelity using moderate laser power ( $f/2\pi \sim 9 \text{ kHz}$ ).

*Limitations.*—Our analytical results have been simplified by dropping  $\hat{H}_{\text{CR}}$  in Eq. (5). However, when the RWA breaks down the enhancement due to PA can no longer be understood simply in terms of the quadrature squeezing  $\mathcal{S}$ . Energy shifts of the Bogoliubov modes due to  $\hat{H}_{\text{CR}}$  can

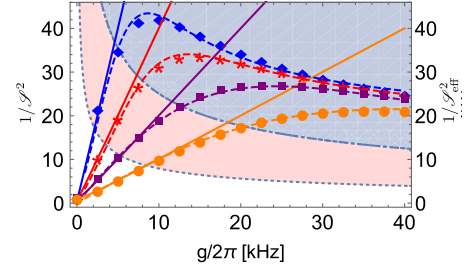


FIG. 4. Breakdown of the rotating wave approximation. The enhancement factors  $1/\mathcal{S}^2$  (solid lines) and  $1/\mathcal{S}_{\text{eff}}^2$  (points, with dashed lines as guides to the eye) as a function of  $g$  for different  $\tau = 2\pi/\delta' \approx (2\pi/g)/(2\mathcal{S}^2)$  at 4, 2, 1, 0.5 ms from left to right. The dotted region (red shaded) corresponds to  $\Delta\delta'_m \geq \delta'_m/20$  and the dot-dashed region (blue shaded) corresponds to  $\Delta\delta'_m \geq \delta'_m/2$ .

be calculated in second-order perturbation theory as  $\Delta\delta'_m = (g_m/\mathcal{S}_m)^2/(4\mu)$ , and can be ignored as long as  $\Delta\delta'_m \ll \delta'_m$  [25], providing a necessary condition for the validity of the RWA. To assess the validity of the RWA more quantitatively, we compare  $\mathcal{S}$  with the effective degree of squeezing  $\mathcal{S}_{\text{eff}}$ . In Fig. 4, we plot both  $1/\mathcal{S}_{\text{eff}}^2$  and  $1/\mathcal{S}^2$  as a function of  $g$  for different values of the time  $\tau$  for a single-loop gate with  $\omega_1/2\pi = 3.045 \text{ MHz}$ . As expected, we observe that they agree very well for small enhancement, deviating appreciably only once  $\Delta\delta'_m = \delta'_m/2$  (dot-dashed region). Note that the maximum achievable enhancement increases with increasing  $\tau$ . The above analysis may have implications for the limitations of PA in other systems [19].

The primary technical concerns in implementing PA experimentally are likely to be the uncertainty in the relative phase  $\theta$  between the SDF and the PA, shot-to-shot frequency fluctuations of  $\delta$ , and imperfect control of the interaction time. Controlling the phase of an optical-dipole force has been demonstrated [43] but can be challenging. Nonzero  $\theta$  does not affect the period of a single loop, but it does reduce the geometric phase  $\Phi$  enclosed by that loop, and therefore reduces the resulting spin-spin interaction strength  $J$ . However, we can show that  $J$  depends on  $\theta$  only to second order. For both spin squeezing and two-qubit gates, the figures of merit (squeezing amount and gate fidelity, respectively) scale quadratically with the shift of  $J$  around its maximal ( $\theta = 0$ ) value [25], and therefore depend only quartically on  $\theta$ . Modeling the phase as a zero-mean Gaussian random number with standard deviation  $\sigma_\theta$ , in Fig. 2(c) we show the expected standard deviation in  $\xi_R^2$  for  $\sigma_\theta = 18^\circ$ . Fluctuations of  $\delta$  (due to fluctuations of either  $\mu$  or  $\omega_m$ ) affect the gate fidelity quadratically by modifying the Bogoliubov frequencies  $\delta'_m$  [25]. For the simulation shown in Fig. 3, we estimate that fidelity  $> 99\%$  is still possible with shot-to-shot frequency fluctuations of 0.2 kHz. Imperfect timing control has a similar effect as fluctuations in  $\delta$  on the degree of spin squeezing and the fidelity of two-qubit gates. In Fig. 3 we show that a 1% timing error [4], reduces the gate fidelity by

about 0.3% in the 5-ion system studied. Finally, we note that in the RWA,  $\hat{\mathcal{H}}_T$  [Eq. (5)] and  $\hat{\mathcal{H}}_{\text{SDF}}$  [Eq. (3)] have the same form, implying that the enhancements of PA are insensitive to the temperature of the initial motional state [44] in the Lamb-Dicke regime.

**Outlook.**—To be concrete we have focused on spin squeezing and two-qubit gates, but the techniques described here are likely to have numerous other applications. For example, it should be possible to enhance the creation of deeply oversqueezed (non-Gaussian) spin states, and it may also be possible to improve amplitude sensing of mechanical displacements [45]. Our strategy is not exclusive of other tools in the trapped ion toolbox; for example, it may be possible to use PA in conjunction with dynamical controls over the driving laser to further suppress unwanted spin-motion entanglement in two-qubit gates. Similar to time-dependent control schemes [14–16], we can also utilize stroboscopic parametric driving protocols to optimize the amplification of spin-spin interactions. For example, stroboscopic protocols consisting of alternating applications of a resonant SDF and a resonant PA with large  $g$  can potentially increase the enhancement factor limits from the RWA breakdown.

We thank Justin Bohnet, Shaun Burd, Daniel Kienzler, and Jiehang Zhang for useful discussions. This manuscript is a contribution of NIST and not subject to U.S. copyright. This work was supported by the Assistant Secretary of Defense for Research & Engineering as part of the Quantum Science and Engineering Program.

- 
- [1] J. I. Cirac and P. Zoller, *Phys. Rev. Lett.* **74**, 4091 (1995).
  - [2] R. Blatt and C. F. Roos, *Nat. Phys.* **8**, 277 (2012).
  - [3] D. J. Wineland, J. J. Bollinger, W. M. Itano, F. L. Moore, and D. J. Heinzen, *Phys. Rev. A* **46**, R6797 (1992).
  - [4] C. J. Ballance, T. P. Harty, N. M. Linke, M. A. Sepiol, and D. M. Lucas, *Phys. Rev. Lett.* **117**, 060504 (2016).
  - [5] J. P. Gaebler, T. R. Tan, Y. Lin, Y. Wan, R. Bowler, A. C. Keith, S. Glancy, K. Coakley, E. Knill, D. Leibfried, and D. J. Wineland, *Phys. Rev. Lett.* **117**, 060505 (2016).
  - [6] J. Zhang, G. Pagano, P. W. Hess, A. Kyprianidis, P. Becker, H. Kaplan, A. V. Gorshkov, Z. X. Gong, and C. Monroe, *Nature (London)* **551**, 601 (2017).
  - [7] J. G. Bohnet, B. C. Sawyer, J. W. Britton, M. L. Wall, A. M. Rey, M. Foss-feig, and J. J. Bollinger, *Science* **352**, 1297 (2016).
  - [8] C. Monroe, D. M. Meekhof, B. E. King, W. M. Itano, and D. J. Wineland, *Phys. Rev. Lett.* **75**, 4714 (1995).
  - [9] C. Ospelkaus, U. Warring, Y. Colombe, K. Brown, J. Amini, D. Leibfried, and D. Wineland, *Nature (London)* **476**, 181 (2011).
  - [10] T. P. Harty, M. A. Sepiol, D. T. C. Allcock, C. J. Ballance, J. E. Tarlton, and D. M. Lucas, *Phys. Rev. Lett.* **117**, 140501 (2016).
  - [11] R. Ozeri, W. M. Itano, R. B. Blakestad, J. Britton, J. Chiaverini, J. D. Jost, C. Langer, D. Leibfried, R. Reichle, S. Seidelin, J. H. Wesenberg, and D. J. Wineland, *Phys. Rev. A* **75**, 042329 (2007).
  - [12] H. Uys, M. J. Biercuk, A. P. VanDevender, C. Ospelkaus, D. Meiser, R. Ozeri, and J. J. Bollinger, *Phys. Rev. Lett.* **105**, 200401 (2010).
  - [13] N. C. Brown and K. R. Brown, *Phys. Rev. A* **97**, 052301 (2018).
  - [14] T. Choi, S. Debnath, T. A. Manning, C. Figgatt, Z.-X. Gong, L.-M. Duan, and C. Monroe, *Phys. Rev. Lett.* **112**, 190502 (2014).
  - [15] T. J. Green and M. J. Biercuk, *Phys. Rev. Lett.* **114**, 120502 (2015).
  - [16] P. H. Leung, K. A. Landsman, C. Figgatt, N. M. Linke, C. Monroe, and K. R. Brown, *Phys. Rev. Lett.* **120**, 020501 (2018).
  - [17] D. J. Heinzen and D. J. Wineland, *Phys. Rev. A* **42**, 2977 (1990).
  - [18] M. Babadi, M. Knap, I. Martin, G. Refael, and E. Demler, *Phys. Rev. B* **96**, 014512 (2017).
  - [19] M.-A. Lemonde, N. Didier, and A. A. Clerk, *Nat. Commun.* **7**, 11338 (2016).
  - [20] S. Zeytinoglu, A. Imamoglu, and S. Huber, *Phys. Rev. X* **7**, 021041 (2017).
  - [21] C. Arenz, D. I. Bondar, D. Burgarth, C. Cormick, and H. Rabitz, *arXiv:1806.00444*.
  - [22] A. Sørensen and K. Mølmer, *Phys. Rev. A* **62**, 022311 (2000).
  - [23] D. Leibfried, B. DeMarco, V. Meyer, D. Lucas, M. Barrett, J. Britton, W. M. Itano, B. Jelenković, C. Langer, T. Rosenband, and D. J. Wineland, *Nature (London)* **422**, 412 (2003).
  - [24] J. J. García-Ripoll, P. Zoller, and J. I. Cirac, *Phys. Rev. A* **71**, 062309 (2005).
  - [25] See Supplemental Material at <http://link.aps.org/supplemental/10.1103/PhysRevLett.122.030501> for technical details, which includes Refs. [26,27].
  - [26] G. J. Milburn, S. Schneider, and D. F. V. James, *Fortschr. Phys.* **48**, 801 (2000).
  - [27] D. Dylewsky, J. K. Freericks, M. L. Wall, A. M. Rey, and M. Foss-Feig, *Phys. Rev. A* **93**, 013415 (2016).
  - [28] C. Ospelkaus, C. E. Langer, J. M. Amini, K. R. Brown, D. Leibfried, and D. J. Wineland, *Phys. Rev. Lett.* **101**, 090502 (2008).
  - [29] J. W. Britton, B. C. Sawyer, A. C. Keith, C.-C. J. Wang, J. K. Freericks, H. Uys, M. J. Biercuk, and J. J. Bollinger, *Nature (London)* **484**, 489 (2012).
  - [30] D. F. James, *Appl. Phys. B* **66**, 181 (1998).
  - [31] D. Porras and J. I. Cirac, *Phys. Rev. Lett.* **92**, 207901 (2004).
  - [32] K. Kim, M. S. Chang, R. Islam, S. Korenblit, L. M. Duan, and C. Monroe, *Phys. Rev. Lett.* **103**, 120502 (2009).
  - [33] In general, the condition is  $|g| < |\delta_m|$ . In this Letter, we assume  $0 < g < \delta_m$  for simplicity.
  - [34] H. Carmichael, G. Milburn, and D. Walls, *J. Phys. A* **17**, 469 (1984).
  - [35] The geometric phase is obtained by numerically solving Eq. (5), and extracting the area enclosed by the phase-space

trajectories in the interaction picture of the total quadratic terms.

- [36] G. Tóth, C. Knapp, O. Gühne, and H. J. Briegel, *Phys. Rev. Lett.* **99**, 250405 (2007).
- [37] J. Ma, X. Wang, C.-P. Sun, and F. Nori, *Phys. Rep.* **509**, 89 (2011).
- [38] D. J. Wineland, J. J. Bollinger, W. M. Itano, and D. J. Heinzen, *Phys. Rev. A* **50**, 67 (1994).
- [39] M. Kitagawa and M. Ueda, *Phys. Rev. A* **47**, 5138 (1993).
- [40] M. Foss-Feig, K. R. A. Hazzard, J. J. Bollinger, and A. M. Rey, *Phys. Rev. A* **87**, 042101 (2013).
- [41] R. J. Lewis-Swan, M. A. Norcia, J. R. K. Cline, J. K. Thompson, and A. M. Rey, *Phys. Rev. Lett.* **121**, 070403 (2018).
- [42] For consistency with the experiment reported in Ref. [7], in the numerical simulations we include the effects of both spontaneous spin flips and additional elastic dephasing, reporting the combination of these two rates as  $\Gamma$  in Fig. 2.
- [43] C. T. Schmiegelow, H. Kaufmann, T. Ruster, J. Schulz, V. Kaushal, M. Hettrich, F. Schmidt-Kaler, and U. G. Poschinger, *Phys. Rev. Lett.* **116**, 033002 (2016).
- [44] K. Mølmer and A. Sørensen, *Phys. Rev. Lett.* **82**, 1835 (1999).
- [45] K. A. Gilmore, J. G. Bohnet, B. C. Sawyer, J. W. Britton, and J. J. Bollinger, *Phys. Rev. Lett.* **118**, 263602 (2017).